frontiers | Frontiers in Nanotechnology

TYPE Original Research
PUBLISHED 17 April 2025
DOI 10.3389/fnano.2025.1578620

OPEN ACCESS

EDITED BY
Shu Zhang,
Nanjing Forestry University, China

REVIEWED BY
Wenran Gao,
Nanjing Forestry University, China
Tasrin Shahnaz,
Universiti Tenaga Nasional, Malaysia

*CORRESPONDENCE
Jyotsana Mehta,
jyotsanamehta1@gmail.com
Bunushree Behera,
bunushree.behera@thapar.edu

RECEIVED 18 February 2025
ACCEPTED 03 April 2025
PUBLISHED 17 April 2025

CITATION
Sikri N, Kumar S, Behera B and Mehta J (2025) Graphene oxide/layered double hydroxide composite as highly efficient and recyclable adsorbent for removal of ciprofloxacin from aqueous phase.
Front. Nanotechnol. 7:1578620.
doi: 10.3389/fnano.2025.1578620

Graphene oxide/layered double hydroxide composite as highly efficient and recyclable adsorbent for removal of ciprofloxacin from aqueous phase

Nidhi Sikri[1], Sandeep Kumar[2], Bunushree Behera[1]* and Jyotsana Mehta[1]*

[1]Department of Biotechnology, Thapar Institute of Engineering and Technology, Patiala, Punjab, India, [2]Department of Physics, Punjab Engineering College (Deemed to be University), Chandigarh, India

Antibiotics, although developed for curing bacterial infections, contaminate the environment, and their long-term unintentional exposure has detrimental effects on the environment, human health, and other organisms, leading to antibacterial resistance, genotoxicity, birth deformities, inhibition of cell proliferation, and reduction of photosynthetic activity. Therefore, there is a compelling need to remove antibiotic contaminants from water reservoirs, and nano-platforms are emerging as attractive platforms for environmental remediation. In this regard, a composite of graphene oxide (GO) with ZnAlNi layered double hydroxide (LDH) has been explored for highly efficient adsorptive removal of priority antibiotic, ciprofloxacin (CIP). The composite containing ZnAlNi-LDH with specific removal capability towards CIP and GO displaying high surface area for adsorption has been synthesized using the co-precipitation method followed by hydrothermal aging. The formed adsorbent has been structurally characterized using several analytical instrumentation techniques demonstrating its potential for antibiotic adsorption. The adsorption of CIP onto GO-ZnAlNi LDH has been studied by varying several parameters including contact time, pH, adsorbent, and adsorbate concentration. The composite demonstrated more than 80% removal of CIP at 1 mg/L initial concentration from the aqueous solution in 1 h with 10 mg/L adsorbent at pH 7. The kinetics of adsorption fits well with pseudo-first-order model, Elovich model and equilibrium adsorption capacity of 106.97 mg/g was obtained. The composite platform also exhibited high stability, regeneration, and reusability up to five cycles.

KEYWORDS

antibiotic, adsorption, ciprofloxacin, graphene oxide, layered double hydroxides

1 Introduction

The rapid growth of industries and the expanding population are driving increased pollution through excessive resource consumption and waste generation (Sharma et al., 2020). This waste includes the presence of various antibiotics as contaminants in the aqueous solution. Antibiotics are biologically active compounds designed to cure bacterial infections in both humans and animals (Kovalakova et al., 2020). A significant portion of ingested antibiotics is excreted through urine. Around 70% of excreted antibiotics find their

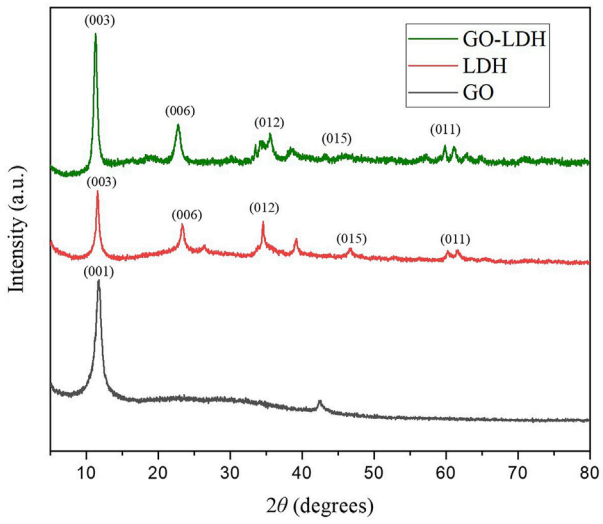

FIGURE 1
XRD pattern of prepared GO, ZnAlNi LDH and GO-ZnAlNi LDH composite.

way into sewage wastewater, where they persist and affect the environment (Chaturvedi et al., 2021; Phoon et al., 2020). Fluoroquinolones are the recalcitrant antibiotic class, which cannot be biodegraded to low and notable concentrations (Wang et al., 2016). Among these, removal of ciprofloxacin from the wastewater system is challenging due to its high solubility and high stability in aqueous solutions. Dixit et al. (2024) investigated the presence and distribution of ciprofloxacin (CIP) i.e. (50–100 μgL^{-1}), with other frequently used pharmaceuticals including norfloxacin, cetirizine, citalopram oxalate in the Sirsa River water in the Baddi-Barotiwala-Nalagarh region of Indian Himalayas, along with the associated ecological and human health risks. Such high concentrations of CIP can lead to various adverse effects on human health, including bacterial resistance as well as symptoms such as vomiting, diarrhoea, leucopenia, and stomatitis (Khan et al., 2020). Methods like advanced oxidation have the capability to break down antibiotic molecules into simpler compounds or even completely mineralize them. However, implementing these processes on an industrial scale proves to be extremely costly and challenging (Ahmed et al., 2015). In such cases, adsorption proves itself an efficient alternative because of its low cost with high efficiency, low energy demand, simple operation, and without secondary pollution (Shahnaz et al., 2022). Among various adsorbents, graphene oxide (GO) is preferred because of its high specific surface area, porosity, and strong interactions (Yu et al., 2016). GO exhibits a layered structure composed of individual graphene sheets. These sheets consist of a hexagonal lattice of carbon atoms bonded together in a two-dimensional honeycomb arrangement (Sun, 2019). It possesses various oxygen functionalities, including carbonyl (C=O), carboxyl (-COOH), epoxy (C-O-C), and hydroxyl (-OH) groups. These groups have the capability to establish complexes with diverse metal ions and organic contaminants through coordination, hydrogen bonding, and electrostatic interaction mechanisms (Singh et al., 2023). Moreover, the oxygen-containing groups contribute to widening the interlayer space within graphene oxide. This facilitates functionalization through the insertion of small molecules or polymers. This enables various modifications for its application in water purification, including the adsorption of antibiotics (Yu et al., 2016).

LDHs are distinctive brucite-like materials characterized by alternating layers of divalent and trivalent metal hydroxides, with anions located in the interlayer spaces. The general formula for these compounds is $[M_{1-x}^{2+}M_x^{3+}(OH)_2]^{x+}$ $[(A^{n-})_{x/n}\cdot mH_2O]$; where M^{2+} and M^{3+} are divalent and trivalent metal cations, respectively, and A^{n-} is an n-valent anion (Priyanka et al., 2024). LDH find its use in various areas including electrochemistry, catalysis, photochemistry, and environmental applications. In addition, LDH can be combined with other carbon nanostructures, including GO, to obtain specialized LDH with improvement in surface and adsorption properties (Feng et al., 2022).

In previous studies, Radmehr et al. (2021), synthesized graphene oxide-based adsorbent [NiZrAl-layered double hydroxide-graphene oxide-chitosan (NiZrAl-LDH-GO-CS NC)] for the effective adsorptive removal of nalidixic acid. Prepared composite presented more than 90% of nalidixic acid removal following pseudo second-order kinetic model (Radmehr et al., 2021). A large surface area of Mg-Al-layered double hydroxides/Activated carbon (Mg-Al-LDH/AC) nanocomposite for the adsorption of tetracycline under an aqueous environment has shown an adsorption capacity of 106.4 mg/g for tetracycline via incorporation of 20% by weight of activated carbon into LDH (Khorshidi et al., 2023). Similarly, Tao et al. (2020) studied that adsorption of levofloxacin hydrochloride on composite of cellulose nanocrystals/graphene oxide was through π-π bond stacking, hydrogen bonding and electrostatic attraction, with removal efficiency exceeding 80.1% (Tao et al., 2020). MgAl-LDH prepared using co-precipitation method was explored for the adsorption of amoxicillin. The adsorption of amoxicillin followed pseudo second-order kinetics indicating that the primary mechanism is predominantly chemisorption (Elhaci et al., 2021). Ai et al. (2019) explained that π-π interactions are the major driving force responsible for the adsorption of tetracycline on GO and hydrogen bonds were found primarily in the GO-tetracycline system.

Most of the research studies investigated the adsorption of antibiotics at very high concentration levels. However, a good adsorbent must be able to adsorb even trace or minimal concentration of antibiotic. Thus, to address this gap, the present work focuses on developing a sensitive and adsorption-specific LDH-modified GO adsorbent. To the best of authors' knowledge, the prepared ZnAlNi-LDH doped GO has not been reported for the highly specific and efficient adsorption of CIP. The selection of GO and the metal combinations in LDH were guided by their cost-effectiveness and easy accessibility of raw materials along with specificity, reusability, and environmental suitability of adsorbent. The GO-ZnAlNi LDH composite was synthesized through co-precipitation, followed by hydrothermal ageing. The adsorbent was well characterized in terms of its surface morphology, functionality, elemental composition, crystallinity and thereafter, different parameters (pH, adsorbate and adsorbent concentration) influencing CIP adsorption were evaluated. The underlying mechanism for adsorption of CIP on the GO-LDH composite

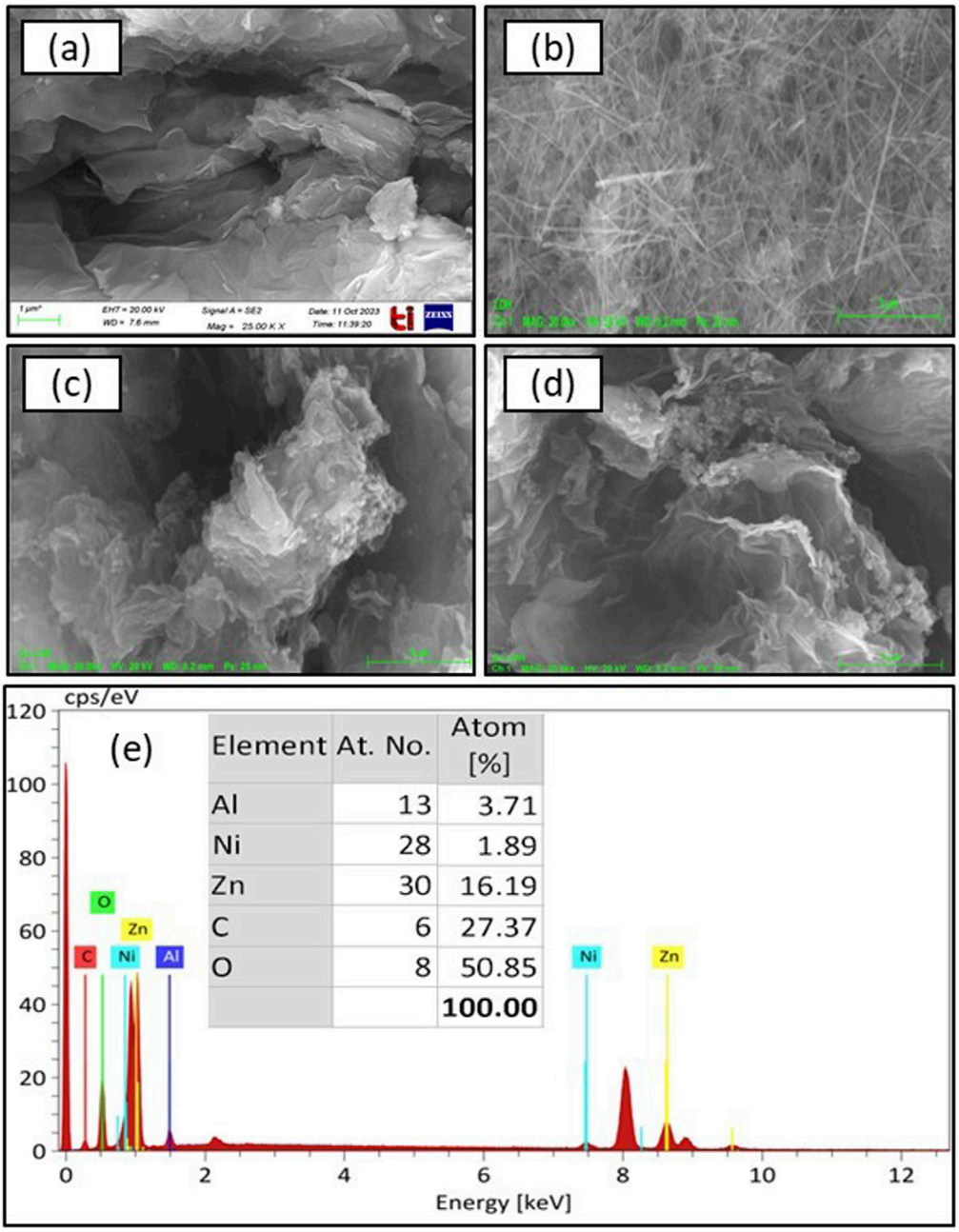

FIGURE 2
SEM images of **(a)** GO, **(b)** ZnAlNi LDH, **(c–d)** GO-ZnAlNi LDH composite, and **(e)** EDX spectra of GO-ZnAlNi LDH composite.

was studied by fitting the data into kinetic and isotherm models. The regeneration studies were also carried out to understand the stability and efficiency of adsorbent during multiple cycles.

2 Material and methods

2.1 Chemicals and reagents

Graphite synthetic 97% pure (Type 2) (100 mesh), Nickel nitrate hexahydrate [Ni $(NO_3)_2.6H_2O$] (99%), Sodium hydroxide pellets, Zinc nitrate hexahydrate [Zn $(NO_3)_2.6(H_2O)$] (99%) were purchased from Sisco research laboratory, India. Aluminium nitrate nonahydrate [Al $(NO_3)_3.9H_2O$] (98%) was purchased from Loba Chemie Pvt. Ltd (India). Ciprofloxacin Hydrochloride [$C_{17}H_{18}FN_3O_3$.HCl (H_2O)] (≥95%) was purchased from Cayman Chemical Company, United States.

2.2 Synthesis of ZnAlNi-LDH

ZnAlNi LDH was prepared by dissolving metal ion solution containing a mixture of 6 mM Zn $(NO_3)_2.6H_2O$, 3 mM of Al (NO_3)

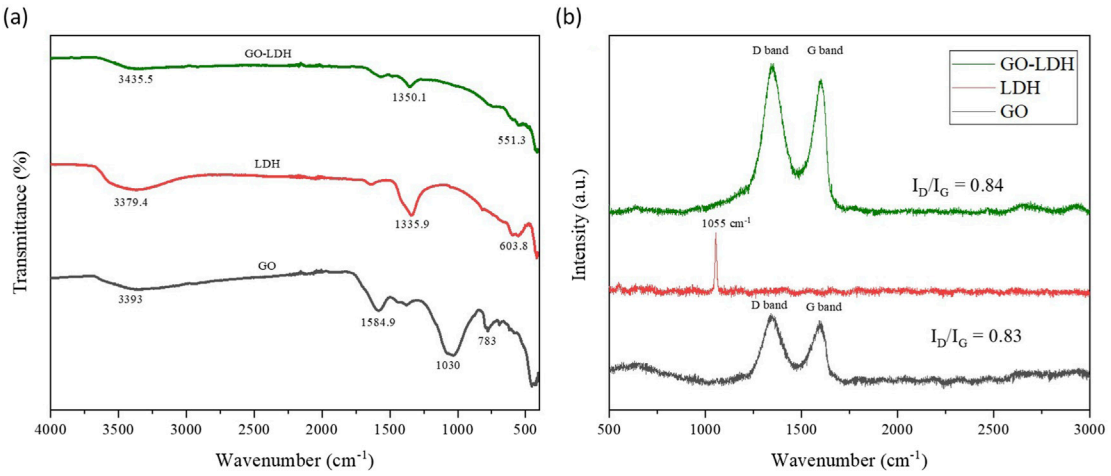

FIGURE 3
(a) Raman spectra and **(b)** FTIR pattern of prepared GO, ZnAlNi LDH and GO-ZnAlNi LDH composite.

$_3$.9H_2O and 1 mM of Ni $(NO_3)_2$.6H_2O in distilled water (solution 1). Metal ion solution was added dropwise to a 30 mL solution containing 0.05 mM Na_2CO_3. The pH of the resulting mixture was kept at 10 by dropwise addition of 3.4 M NaOH to ensure optimal hydroxylation, promoting the formation of stable brucite-like layers, and preventing metal ion precipitation. This pH also maintains a balanced anion exchange environment, crucial for structural integrity of LDH. Finally, the reaction mixture was hydrothermally treated at 120°C for 16 h. After hydrothermal treatment, the materials were filtered and washed with distilled water and ethanol until supernatant becomes neutral. At last, sample was dried at 70°C in a hot-air oven (Deng et al., 2021).

2.3 Synthesis of GO and GO-ZnAlNi LDH composite

GO was prepared using modified hummers method (Guerrero-Contreras and Caballero-Briones, 2015). For the synthesis of GO-ZnAlNi LDH, GO (500 mg) was added to distilled water and dispersed by ultrasonication for 1 h. Prepared GO suspension was mixed with Solution 1 for 30 min, followed by its addition into a 30 mL solution containing 0.05 mM Na_2CO_3. pH of the solution mixture was kept at 10 by addition of 3.4 M NaOH. Lastly, solution mixture was treated hydrothermally at 120°C for 16 h. After treatment, final sample was collected and washed with distilled water and ethanol until effluent becomes neutral. Finally, the sample was dried at 70°C in hot air oven (Deng et al., 2021).

2.4 Characterization of GO and GO-ZnAlNi LDH composite

The nano-adsorbent was characterized by X-ray diffraction (XRD) patterns using Cu-Kα (1.54 Å) with diffraction angle (2θ = 0°–90°) (Smart Lab, SE model) for the determination of crystal structure and material phase identification. Fourier transform infrared spectroscopy (FTIR) spectra was studied for detecting the functional groups and vibrations of chemical bond with frequency range from 400–4,000 cm^{-1}. Microstructure of nano-adsorbent, morphological characterization and surface elemental composition were determined using a field emission scanning electron microscope (FE-SEM, Carl Zeiss Sigma 500 model) equipped with energy dispersive X-ray spectroscopy. Vibrational modes were determined using Raman Spectra (Labram HR confocal micro-Raman Spectrophotometer). The surface area of prepared composite was determined by using Brunauer Emmett Teller (BET) Surface Analyzer.

2.5 Batch experimentation with adsorbent

The adsorption performance of nano-adsorbent was analyzed under various parameters, including the concentration of ciprofloxacin (0.225 mg/L to 10 mg/L), a dose of adsorbent (1 mg/L to 12 mg/L), pH of the solution (3–11) with contact time ranging between 0 min and 4 h. The experiment was set up in a beaker with 20 mL volume containing ciprofloxacin and adsorbent with continuous stirring at 180 rpm. The required amount of mixture was then taken at regular intervals and centrifuged at 10000 rpm for 5 min. The collected supernatant was utilized for analyzing the CIP concentration using optical density measurements via UV-Vis spectrophotometer at 276 nm using calibration curve (Supplementary Figure S1).

The removal efficiency of CIP adsorption (%) was calculated according to Equation 1.

$$Removal\ efficiency\ (\%) = \frac{(C_o - C_t)}{C_o} \times 100 \quad (1)$$

where C_o and C_t are the initial and final concentrations of CIP (mg/L) respectively.

The adsorption capacity (q_t) of adsorbent (mg/g) was calculated using the following Equation 2

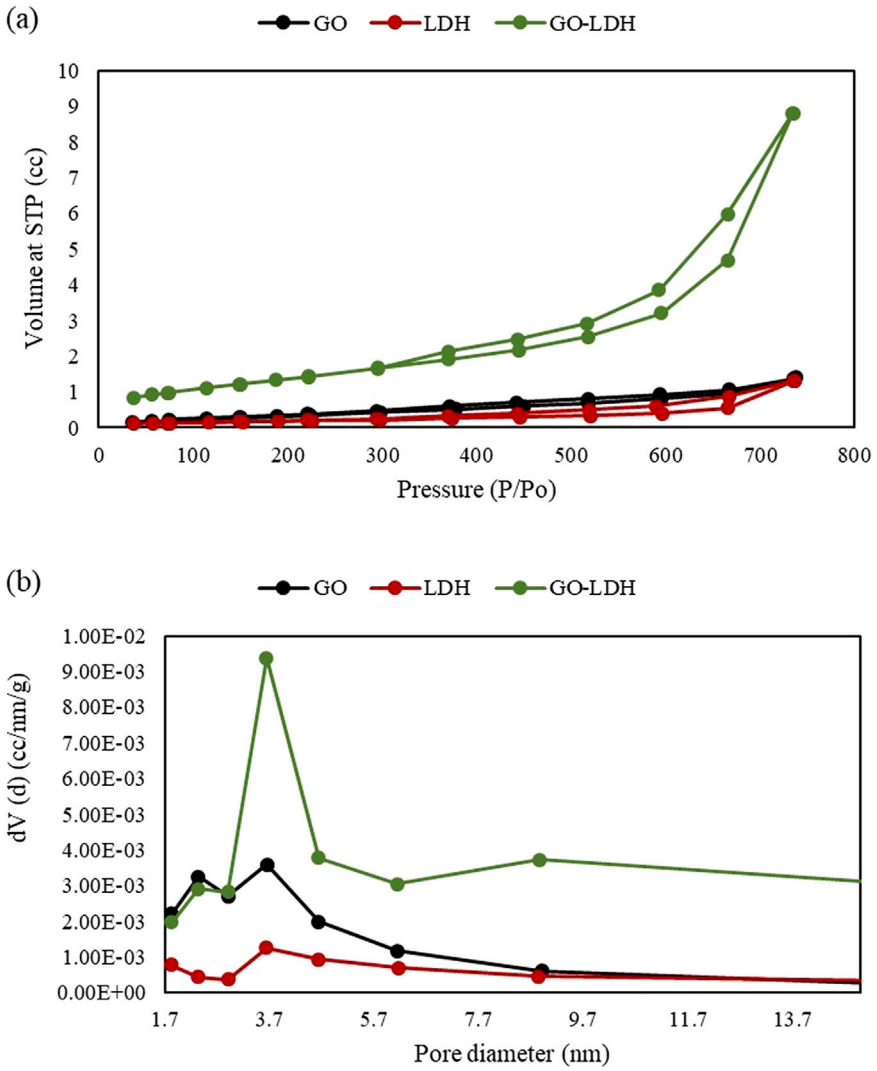

FIGURE 4
(a) N_2 adsorption-desorption isotherm and **(b)** pore size distribution of GO, ZnAlNi LDH and GO-ZnAlNi LDH composite.

$$q_t = \frac{(C_o - C_t)V}{W} \quad (2)$$

where q_t is the adsorption capacity (mg/g) of adsorbent at time t, C_o. and C_t are the initial and final concentrations of CIP (mg/L) at time t, respectively, in the solution. V is the volume of stock solution (L), and W is the amount of adsorbent GO-ZnAlNi LDH (g).

2.6 Reusability of GO-LDH composite

The reusability of adsorbents plays a vital role in practical applications concerning their overall stability (Shahnaz et al., 2020). In this study, desorption experiments were conducted on the CIP-loaded GO-ZnAlNi LDH composite to assess its performance. Distilled water was utilized as the desorption solvent to study the desorption rate of CIP. Following the adsorption process, the GO-ZnAlNi LDH composite was separated through centrifugation and subjected to three rounds of washing with distilled water for a specific duration to facilitate desorption. Adsorption was then performed under the optimal combination of parameter and the removal efficiency was estimated. Finally, the adsorbent was centrifuged again and dried, completing one adsorption-desorption cycle.

3 Results and discussion

3.1 Structural characterization of GO-LDH composite

3.1.1 XRD analysis

The XRD patterns were used to determine the crystal structure of GO, ZnAlNi LDH and GO-ZnAlNi LDH composite as shown in Figure 1. The XRD spectra were measured in a range from 5° to 80°. The high intensity at (003), (006) and (012) indicated that the synthesized LDH showed a high degree of crystallinity. The

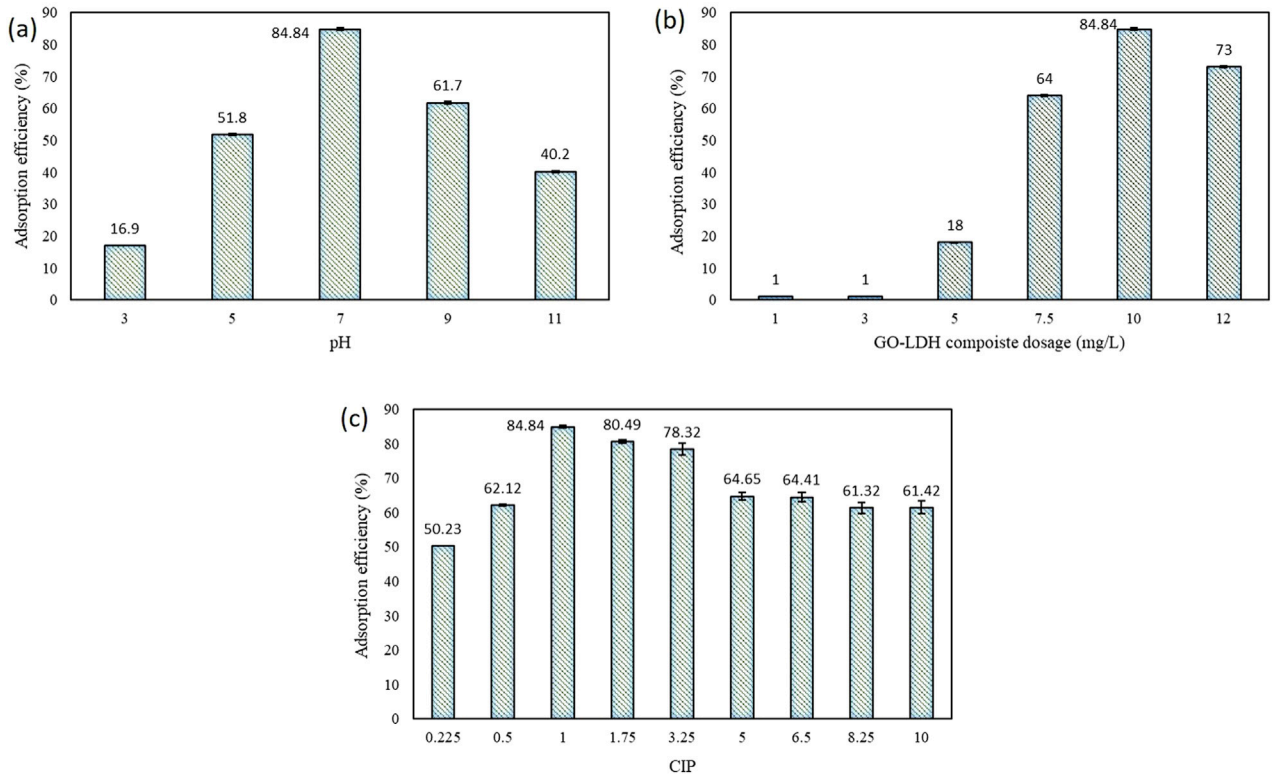

FIGURE 5
(a) Effect of pH **(b)** adsorbent dosage and **(c)** CIP concentration on adsorption onto prepared composite.

diffraction peaks of GO were observed at 11.48°, which corresponds to the (001) lattice plane, indicating complete oxidation of graphite powder into GO (Hidayah et al., 2017; Stobinski et al., 2014). The basal diffraction peaks of ZnAlNi LDH were found at 11.02°, 23.06°, and 35.02°, referring to the planes (003), (006), (012) attributed to the regular layered structure with rhombohedral symmetry (Bezerra et al., 2021). GO-ZnAlNi LDH composite showed a series of significant diffraction peaks at diffraction angles (2θ) of 11.34°, 23.64°, 34.93°, 46.96° and 61.1° which corresponds to the lattice planes (003), (006), (012), (015) and (110), respectively representing the brucite like layer with high crystallinity.

3.1.2 FE-SEM and EDX analysis

Morphological and structural properties, along with the surface elemental composition of GO, ZnAlNi LDH and GO-ZnAlNi LDH composite, were studied using FE-SEM and EDX analysis, as represented in Figure 2. The SEM micrographs of synthesized GO (Figure 2a) from modified hummers method showed layered structure, including ultrathin and homogeneous films. These thin films were folded or continuous at times. In addition, individual sheets could be distinguished easily. Flaky thin sheets indicated the oxidation of graphene into GO (Alicanoglu & Sponza, 2017). The surface characteristics of ZnAlNi LDH as in Figure 2b, showed uneven aggregates with long rod like structure with dendritic apertures (Kanimozhi et al., 2023). The GO-ZnAlNi LDH composite exhibited sandwich like layered structure (Figures 2c,d). Similar type of structure has also been observed by Priyanka et al. (2024). Such morphology provides beneficiaries for the adsorbate molecule facilitating better adsorption. Additionally, the elemental analysis of the GO-ZnAlNi LDH composite represented in Figure 2e revealed that carbon (27%) and oxygen (50%) were the primary constituents, while the remaining composition consisted of zinc, aluminum and nickel ions at 16.19%, 3.71%, and 1.89%, respectively.

3.1.3 FTIR analysis

FTIR spectrum, as shown in Figure 3a of prepared GO, ZnAlNi LDH and GO-ZnAlNi LDH composite, was used to identify the vibrational properties of functional groups. The FTIR spectrum of GO showed a sharp peak at 3393 cm^{-1}, corresponding to hydroxyl group bending due to the presence of water molecules. The peaks 1584.9 cm^{-1} and 1379.4 cm^{-1} occurred due to C=C stretching of cyclic alkene along with unoxidized graphitic domains due to sp^2 hybridization and bending mode of the hydroxyl group (–C–OH) over the basal plane. Other significant bands were located at 1030 cm^{-1} corresponding to the epoxy (C–O–C) stretching over the basal plane of GO. The band observed at 783 cm^{-1} corresponded to the–C–H bending (Guerrero-Contreras and Caballero-Briones, 2015). Similarly, the FTIR spectrum of ZnAlNi LDH showed a peak at 3379.4 cm^{-1} confirming –OH stretching vibrations due to interlayer water molecules. Another peak at 1335.9 cm^{-1} was attributed to –OH bending vibrations and carbonate (CO_3^{2-}) ions in the interlayer of LDH. Further, the peak observed at 603.8 cm^{-1} was because of –C=C–alkene bonding. Any absorption bands observed under 800 cm^{-1} could be described for the metal-oxygen bonding (M–O–M, M–O, O–M–O) (Rahman and Raheem, 2022).

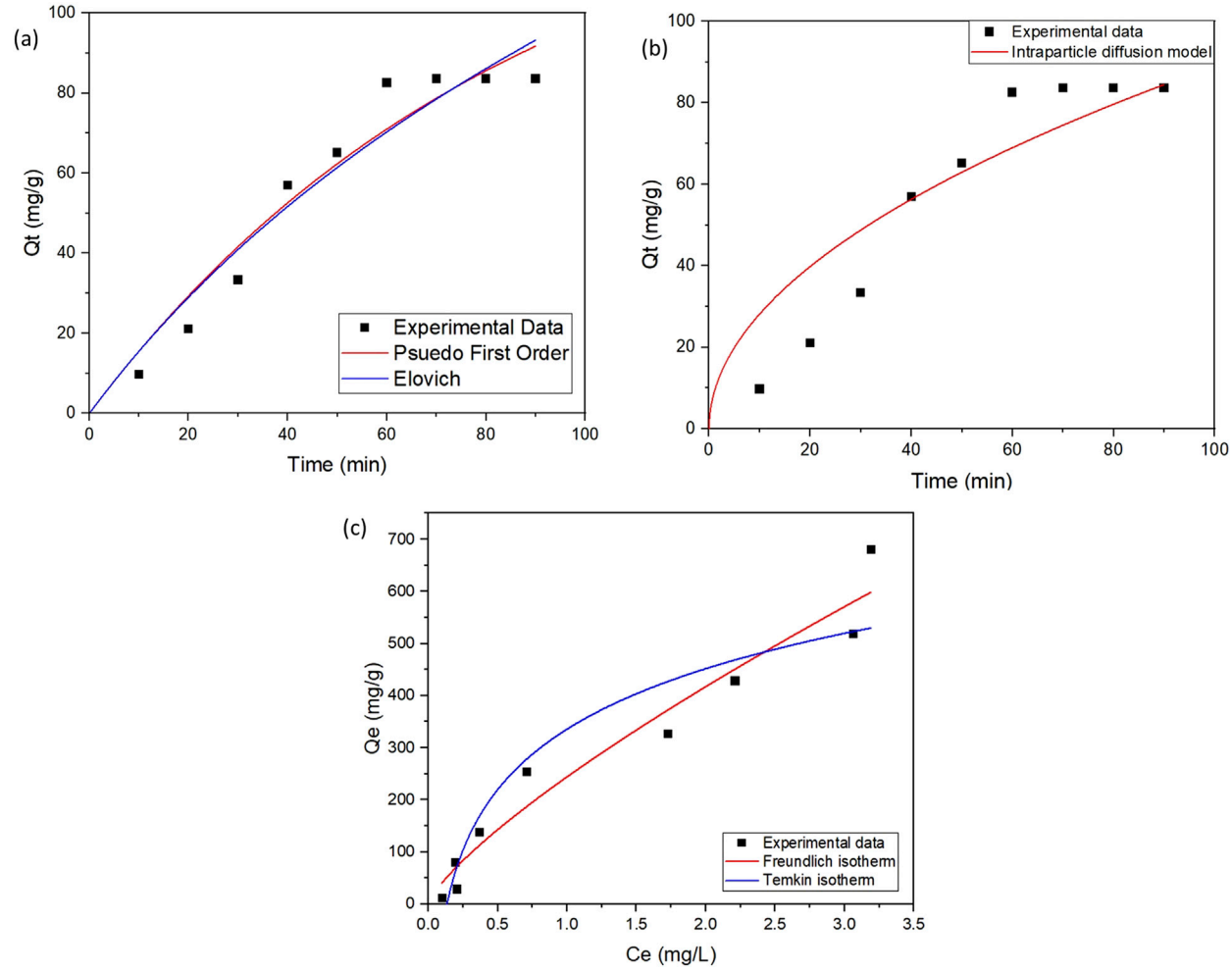

FIGURE 6
(a) Pseudo-first order and Elovich model **(b)** Intra-particle diffusion model and **(c)** Isotherm modeling for adsorption of CIP on GO-LDH composite under equilibrium conditions.

In GO-ZnAlNi LDH composite, peaks at 3435.3 cm^{-1} and 1350.1 cm^{-1} confirmed the –OH bending vibrations due to the presence of water molecules and carbonate (CO_3^{2-}) ions in the interlayer of LDH, respectively. Additionally, the peak observed at 551.3 cm^{-1} described the metal-oxygen bonding, further confirming the formation of GO-ZnAlNi LDH composite (Deng et al., 2021).

3.1.4 Raman and BET surface area analysis

Raman spectroscopy was employed to examine the vibrational energy modes of GO, ZnAlNi LDH, and GO-ZnAlNi LDH composite (Figure 3b). In the case of GO, vibrational modes were identified within the spectral range of 1,300 cm^{-1} to 1,600 cm^{-1}. Specifically, the D band was observed at 1,350 cm^{-1}, while the G band was noted at 1,598 cm^{-1} (Zhou et al., 2019). Conversely, the ZnAlNi LDH exhibited vibrational modes at 1055 cm^{-1}. The presence of peaks at 1,055 cm^{-1}, 1,350 cm^{-1}, and 1598 cm^{-1} serves as evidence for the successful synthesis of the GO-ZnAlNi LDH composites as also reported by Priyanka et al. (2024). Furthermore, the lower intensity of the G band compared to D in the composite indicated well lamellar structure because of the deposition of LDH on the sheet-like structure of GO (Bu et al., 2020). Figure 4a represents the N_2 adsorption-desorption isotherm of ZnAlNi LDH and GO-ZnAlNi LDH composite. All materials produced type IV isotherms as represented by distinct adsorption-desorption peaks. Similar kinds of isotherms were also observed for GO@NiAl LDH composite by Priyanka et al. (2024). Figure 4b described the incremental pore volume curves of the materials with multi-modal peaks. The materials exhibited microporous structure with a pore volume of 0.021, 0.014 and 0.098 cc/g for GO, ZnAlNi LDH and GO-ZnAlNi LDH composite, respectively. The surface area of ZnAlNi LDH and GO-ZnAlNi LDH was found to be 6.197 m^2/g and 38.069 m^2/g, respectively. GO has been reported to significantly enhance the surface area of LDH via the complexation of its negative functional groups over cations of the latter material (Rashed et al., 2022).

3.2 Influence of operational parameters on adsorption efficiency

3.2.1 Effect of pH on CIP adsorption efficiency

The pH of a solution often influences both the speciation of CIP and the surface functional groups present on the composite material

TABLE 1 Kinetic model parameters for sorption of CIP on GO-LDH composite.

Kinetic models with regression coefficients	Parameters
Pseudo-first order model (R^2 = 0.949)	qe = 106.96 mg/g; k_1 = 0.014
Elovich model (R^2 = 0.945)	α = 4.09, β = 0.03
Intra-particle diffusion model (R^2 = 0.88)	K_{id} = 0.08, C = 2.01

TABLE 2 Kinetic parameters for adsorption of CIP on GO-LDH composite under equilibrium conditions.

Parameters	Values
Freundlich Isotherm Model	
N	1.29
K_f	244.32
R^2	0.95
Temkin Isotherm Model	
A_T (L/mg)	7.4
B_T (J/mol)	167.3
b_T	15.06
R^2	0.90

(Zhu et al., 2015). Therefore, it is crucial to examine the impact of pH on the adsorption process. A batch adsorption experiment was performed with 1 mg/L concentration of CIP under acidic, neutral and alkaline pH (3, 5, 7, 9, and 11), revealing their role in the adsorption process (Figure 5a). The effects of pH were studied at an adsorption time of 1 h at a GO-ZnAlNi LDH composites concentration of 10 mg/L. The removal efficiency of CIP increased with pH, reaching its highest rate at pH 7, after which it started to decline. CIP, being a zwitter ionic compound with two pKa values (pKa1 = 6.1 and pKa2 = 8.7), exists in a cationic form at pH values below 6.1 and in an anionic form at pH values above 8.7 (Wang et al., 2016). At lower pH, CIP primarily exists as a cation; however, as the pH increases, the reduction in its cationic form minimizes electrostatic repulsion, thereby enhancing adsorption capacity, which rises from 6.15 mg/g at pH 3–56.41 mg/g at pH 5 (Zhu et al., 2015). Between pH 6.1 and 8.7, when CIP is zwitter ionic, the adsorption process is more favourable, maximum removal efficiency and adsorption capacity of 84.84% and 97.43 mg/g respectively were observed. Similar to the present study, maximum adsorption efficiency was observed at pH seven for CIP using nano graphene oxide magnetite composite (Alicanoglu and Sponza, 2017). As the pH increased from 9 to 11, the electrostatic repulsion between the adsorbent surface and CIP intensified, reducing the adsorption capacity from 69.74 mg/g to 22.56 mg/g. Similarly, decreasing patterns of adsorption capacity with respect to increase in pH has also been observed during the adsorption of CIP by zinc ion cross-linked GO and sodium alginate aerogel microspheres (Li et al., 2021).

3.2.2 Effect of adsorbent dosage on CIP adsorption efficiency

The amount of adsorbent dose, which impacts the number of available active sites, is a crucial factor that influences the adsorption process. In this study, the impact of varying adsorbent dose on the adsorption of CIP (1 mg/L) was analyzed by incrementing the adsorbent dose from 1 to 12 mg/L. As represented in Figure 5b, initially, at a concentration up to 3 mg/L, no significant adsorption and constant adsorption capacity, i.e. 10.26 mg/g, of CIP was observed. This might be attributed to the lesser availability of sufficient adsorption sites. Increasing the amount of adsorbent dose from 5 to 7.5 mg/L, significant enhancement in the removal of CIP from 16% to 64% was observed, which could be due to an increase in the availability of the active adsorption sites. A notable improvement in adsorption capacity of 88.89 mg/g was observed for the removal of CIP. A similar trend was observed, where the adsorption capacity increased with the rising concentration of adsorbent during CIP adsorption by modified graphene oxide with Poly N-vinyl caprolactam (Bahar et al., 2021). A maximum CIP removal efficiency of 84.84% and an adsorption capacity of 97.43 mg/g were observed after 1 h at an adsorbent dosage of 10 mg/L. With a further increase in adsorbent concentration to 12 mg/L, adsorption efficiency declined to 73.86%, which might be due to particle aggregation, that blocks the active sites (Priyanka et al., 2024) Similarly, adsorption capacity also decreased to 77.95 mg/g, because when the adsorbent dose reaches its limit, all active sites on the adsorbent surface become fully occupied (Mohammadi et al., 2020). Consequently, the number of unoccupied active sites rises with higher adsorbent doses (Yasmin et al., 2024).

3.2.3 Effect of initial CIP concentration on adsorption efficiency

The effect of varying CIP concentration (0.225 mg/L to 10 mg/L) on the adsorption efficiency was investigated at an adsorbent dose of 10 mg/L and neutral pH (Figure 5C). A gradual increase in the removal of CIP was observed with increasing antibiotic concentration. Maximum removal efficiency of 84.84% was observed at 1 mg/L CIP concentration after 1 h. Increasing the CIP concentration to 3.25 mg/L leads to a slight decrease in removal efficiency up to 78.32%. Furthermore, the removal efficiency remains fairly constant after increasing the CIP concentration to 10 mg/L. This summarizes that when the concentration of CIP increased, adsorption decreased significantly. It could be corroborated by the fact that as the availability of active sites is more, the adsorption of CIP molecules also increases (Alicanoglu and Sponza, 2017). While achieving saturation, all of the available active sites are occupied by the CIP molecules, resulting in no further adsorption. Beyond the threshold concentration, further increases in pollutant concentration led to a decrease in adsorption as the number of available active sites became limited (Khan et al., 2020). An increase in CIP concentration was also found to enhance adsorption capacity from 10.76 mg/g to 524.1 mg/g, by reducing mass transfer resistance and facilitating more frequent collisions between antibiotic molecules. This resulted in higher adsorption per unit weight of adsorbent (Parashar et al., 2023).

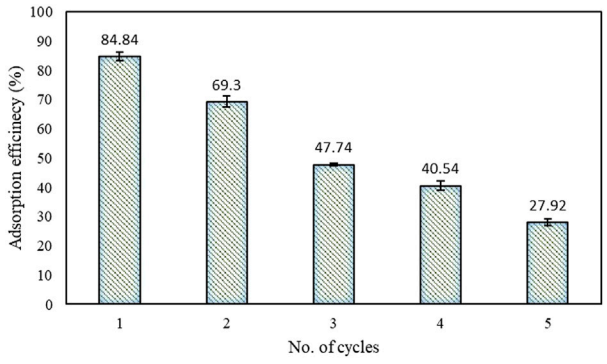

FIGURE 7
Recyclability of GO-ZnAlNi LDH composite.

3.3 Adsorption kinetics of CIP on GO-LDH composite

The adsorption kinetics of CIP onto the GO-ZnAlNi LDH composite were investigated to understand the underlying mechanisms and identify the rate-limiting step. Initially, CIP adsorption onto the composite increased sharply, eventually reaching the maximum adsorption capacity at around 1 h, which afterwards became stable. This equilibrium can be attributed to the significant concentration gradient between the CIP solution and the adsorbent. When the GO-ZnAlNi LDH composite was introduced into the CIP solution, the concentration gradient facilitated the rapid accumulation of CIP on the surface of the adsorbent, followed by its diffusion into the internal structure, leading to maximum adsorption in 1 h. For further investigation, the experimental kinetic data were analyzed by fitting them to pseudo-first-order, pseudo-second-order, Elovich and intraparticle diffusion models. All the equations used for kinetic modelling are non-linear.

Under the concept of the pseudo-first-order kinetic model, the extent of pollutant adsorption is directly proportional to the number of unoccupied sites of adsorbent, which can be expressed by following Equation 3:

$$q_t = q_e\left(1 - e^{-kt}\right) \tag{3}$$

where q_e and q_t represent the adsorption capacities (mg/g) at the equilibrium time and time t (min), respectively; k_1 (1/min) denotes the pseudo-first-order kinetic adsorption rate constant. Further, the pseudo-second-order kinetic model considers the electron exchange between the adsorbent and adsorbate, leading to covalent bond formation. It can be expressed by Equation 4:

$$q_t = \frac{k_2 q_e^2 t}{1 + k_2 q_e^2 t} \tag{4}$$

where k_2 (g/mg min) denotes the pseudo-second-order kinetic rate constant. q_e and q_t represent the adsorption capacities (mg/g) at the equilibrium time and the total adsorption time t (min) respectively.

The Elovich model describes that the rate of adsorption diminishes over time as the surface coverage increases. Such adsorption kinetics can be represented by Equation 5

$$q_t = \frac{\ln(\alpha \cdot \beta t + 1)}{\beta} \tag{5}$$

where q_t represents the adsorption capacities (mg/g) at time t (min), α and β represent the initial adsorption rate (mg/g min) and the desorption constant (g/mg), respectively. Lastly, the intra-particle diffusion model (Equation 6) describes whether diffusion occurs in one or more steps of adsorption, with K_{id} denoting the intraparticle diffusion rate (mg/g $min^{0.5}$) and C representing the constant associated with the effect of film diffusion.

$$q_t = K_{id} \cdot t^{0.5} + C \tag{6}$$

The adsorption data under equilibrium conditions were found to fit the pseudo-first-order model (R^2 = 0.949), Elovich model (R^2 = 0.945) and intra-particle diffusion (R^2 = 0.88) as represented in Figures 6a, b. The relevant kinetic parameters linked with these models are compiled in Table 1. A poor fit was obtained for the pseudo-second-order model. Thus, the adsorption process in the present study appears to involve a combination of complex process mechanisms involving rapid surface adsorption followed by diffusion into the porous structure of the GO-LDH composite. The process can be delineated into three distinct stages: (1) an initial rapid diffusion of CIP onto the surface of the adsorbent, (2) an intra-particle diffusion phase, identified as the rate-limiting step, during which CIP penetrates into the pores of the adsorbent, and (3) equilibrium attainment, characterized by a decline in the intra-particle diffusion rate.

The adsorption of amoxicillin by MgAl LDH was described by both pseudo-first-order (R^2 = 0.979) and pseudo-second-order (R^2 = 0.99) kinetic models (Johnston et al., 2024). Additionally, MgAl LDH modified with vermiculite was found to follow the pseudo-second-order kinetic model, with the intra-particle diffusion model providing further insights into the adsorption behaviour of CIP and tetracycline (Gao et al., 2022). Chen et al. (2021) studied the adsorption of tetracycline onto MOF-525/GO using the Elovich and Sips model, revealing that the adsorption was dominated by chemisorption (Chen et al., 2021).

3.4 Adsorption isotherm modelling for GO-LDH composite

Adsorption isotherm modelling explains the relationship between the quantity of CIP retained on the surface of the adsorbent and its concentration in solution at a constant temperature, discussing detailed adsorption mechanisms, including the interaction forces (Tasrin et al., 2021). Langmuir, Freundlich and Temkin isotherms were applied to analyze the experimental data of the sorption of CIP onto GO-ZnAlNi LDH composite. All the equations used for isotherm modelling are non-linear. The Langmuir isotherm can be expressed by following Equation 7:

$$Q_e = \frac{K_L \cdot Q_m \cdot C_e}{1 + (K_L \cdot C_e)} \tag{7}$$

where C_e represents the liquid-phase equilibrium concentration (mg/L), q_m denotes the maximum adsorption capacity (mg/g), q_e

TABLE 3 Comparative evaluation of equilibrium adsorption capacity for CIP with other adsorbents.

S. No.	Adsorbent	Adsorbate CIP Conc.	Optimum conditions	Adsorption capacity (mg/g)	References
1	GO (5)@NiAL LDH (800–1,000 mg/L)	10 mg/L	pH 6; 180 min	179.2	Priyanka et al. (2024)
2	$MnFe_2O_4$@TiO_2-rGO (200 mg/L)	30 mg/L	pH 5; 60 min	75.88	Chang et al. (2021)
3	Chitosan modified GO (300 mg/L)	40 mg/L	100 rpm; pH 3.5; 210 min	44.843	Parashar et al. (2023)
4	GO-Kaolinite-Poly (vinyl alcohol) (100 mg/L)	20 mg/L	500 min	79.11	Huang et al. (2020)
5	RGO-M (200 mg/L)	5 mg/L	150 rpm; pH 6.2; 24 h	10.89	Tang et al. (2013)
6	GO-ZnAlNi LDH (10 mg/L)	1 mg/L	180 rpm; pH 7; 60 min	106.9	Present work

denotes the equilibrium adsorption capacity (mg/g), and K_L indicates the Langmuir adsorption constant (L/mg).

The Freundlich isotherm is represented by the following Equation 8:

$$q_e = k_f C_e^{1/n} \quad (8)$$

where q_e denotes the equilibrium adsorption capacity (mg/g), C_e represents the equilibrium concentration of adsorbate (mg/L), K_f and n denote Freundlich constants related to the adsorption capacity and adsorption intensity, respectively.

Further, to analyze the heat of adsorption of CIP and GO-LDH composite interactions, the data was also fitted into the Temkin isotherm model as represented in Equation 9.

$$q_e = \frac{RT}{b_T} \ln(A_T C_e) \quad (9)$$

where q_e denotes the equilibrium adsorption capacity (mg/g), C_e represents the equilibrium concentration of adsorbate (mg/L), A_T represents the equilibrium binding constant (L/mg), b_T is the adsorption binding energy (J/mol), and B_T is the adsorption constant often represented in terms of the following Equation 10.

$$B_T = \frac{RT}{b_T} \quad (10)$$

where T is the temperature (K) and R is the universal gas constant (8.314 J/mol. K).

The changes in q_e with increasing CIP concentration were analyzed to evaluate the isothermal parameters of CIP adsorption onto the GO-ZnAlNi LDH composite as represented in Table 2. The adsorption capacities increased progressively with higher CIP concentrations until they reached a saturation point. The equilibrium modelling plots for the adsorption of CIP on GO-LDH composite have been shown in Figure 6c. The adsorption data did not fit significantly with Langmuir isotherm. The Freundlich model provided a better fit for describing the adsorption process among the above-mentioned isotherm models. This suggests that the adsorption occurred primarily through multilayer interactions on the surface of the composite, likely following a site-to-site mechanism. Similarly, Radmehr et al. (2021) also observed the Freundlich isotherm model (R^2 = 0.9997) as the best fit during the adsorption of nalidixic acid using NiZrAl-LDH-GO-chitosan composite. Additionally, the adsorption of azithromycin onto the surface of GO also followed the Freundlich isotherm model (R^2 = 0.998).

With a regression coefficient of 0.90, the data was also found to fit Temkin isotherm modelling, though the regression coefficient achieved was lower than Freundlich isotherm (R^2 = 0.95). The value of the adsorption constant showed positive variation in the adsorption energy parameter with a value of 167.3 J/mol, demonstrating the process to be exothermic. Further, the binding energy reduces linearly with time due to the coverage of GO-LDH composite surface with CIP molecules. Upoma et al. (2022) have shown that azithromycin adsorption onto the waste-derived GO surface was mainly dominated by electrostatic interactions that followed the Temkin model.

3.5 Recyclability and stability of GO-ZnAlNi LDH composite

To evaluate the stability of the GO-ZnAlNi LDH composite, its capacity for reusability in the adsorption of CIP was examined across five consecutive cycles under identical experimental conditions. Following each cycle, the utilised composite was retrieved and employed again in the next batch. The data presented in Figure 7 demonstrate that the maximum CIP removal efficiency of 80.4% was achieved during the initial cycle. Nevertheless, this efficiency exhibited a gradual decline with each subsequent cycle, ultimately reaching 27% by the fifth cycle. These results suggest that the GO-ZnAlNi LDH composite maintains its adsorption capability for CIP across multiple cycles, thereby proving effective in the removal of low-concentration pollutants. GO-cellulose nanofiber composite can also be reused efficiently for up to five regeneration cycles during the adsorption of various forms of tetracycline (Wang et al., 2017). A similar type of recyclability result has also been observed during the adsorption of CIP by halloysite nanotubes/GO composite (Wang et al., 2022). The composite was further analyzed using XRD both before and after adsorption to assess its stability (Supplementary Figure S2). It was observed that the composite maintained an intact crystal structure, which signifies its overall stability.

3.6 Adsorption mechanism of CIP onto GO-ZnAlNi LDH composite

The adsorption mechanism of CIP onto the GO-ZnAlNi LDH composite was investigated through analysis of changes in the adsorbent surface functional properties. The FTIR spectra obtained from the composite before and after the adsorption of CIP exhibited notable alterations. Initially, a peak at 3407 cm^{-1}, associated with -OH bending vibrations, was detected. Following the adsorption process, this peak diminished and ultimately vanished, suggesting that hydroxyl groups played a crucial role in the adsorption mechanism. This observation implies the occurrence of hydrogen bonding between the hydroxyl groups of the composite and the polar functional groups present in CIP (Han et al., 2021). Furthermore, the peaks at 1557 cm^{-1} (C=C alkene stretching) and 1364 cm^{-1} (alcohol stretching vibrations) combined, resulted in a distinct peak at 1408 cm^{-1}, which may indicate the presence of π-π interactions. Considering the aromatic ring structure of CIP, it is possible that the π-electrons from CIP engage with the π-electron system of the GO-ZnAlNi LDH composite (Li et al., 2018). Chitosan-modified GO exhibited π-π interaction and hydrogen bonding for the adsorption of CIP (Parashar et al., 2023). The proposed mechanism for the present study also corroborates well with the isotherm modelling showing the adsorption to be a multi-layer phenomenon influenced by the surface properties of the adsorbent along with rapid diffusion across the pores. Notably, a decline in surface area and pore volume of adsorbent from 36.069 m^2/g to 31.836 m^2/g, and from 0.098 cc/g to 0.086 cc/g was also seen following the adsorption of CIP, further confirming the phenomenon.

3.7 Comparison of adsorption capacity for CIP with other adsorbents

Table 3 shows a comparative analysis of the equilibrium adsorption capacities of various adsorbents for CIP removal. A review of the existing literature reveals that numerous adsorbents have been employed for CIP adsorption. A high adsorption capacity of 1968.5 mg/g for 10 mg/L of CIP by GO (5)@NiAL LDH in 180 min of equilibrium time was reported by Priyanka et al. (2024). In another similar study, Li et al. (2018) projected an adsorption capacity of 111.73 mg/g by incorporating magnetic GO/diethylenetriaminepentaacetic acid nanocomposite with 50 mg/L CIP after 24 h. Tang et al. (2013) obtained equilibrium in 24 h with adsorption capacity of 10.89 mg/g during the adsorption of CIP using RGO-M. However, the prepared GO-ZnAlNi LDH composite in the present study exhibits more sensitive adsorption of CIP as compared to other materials. The prepared composite exhibits exceptional adsorption efficiency, removing 1 mg/L of CIP from aqueous solution with just 10 mg/L of adsorbent after 60 min. Its high surface area and functional groups enhance interaction, ensuring superior removal capacity. This remarkable sensitivity outperforms other adsorbents, making it highly effective even at low dosages of antibiotics. The experimental protocol for the adsorbent synthesis and usage did not result in any toxic by-products unlike other remediation techniques. Further, the adsorption is expected to reduce the antibiotic load in wastewater, thereby reducing the environmental impacts. The composite's rapid adsorption kinetics owing to its superior physicochemical properties, along with its reusability potential over multiple cycles highlight its cost-effectiveness for scale up and real-time wastewater treatment. The implementation of such adsorbent systems aligns with global sustainability goals, that is expected to guide environmental policies for pharmaceutical wastewater management.

It is noteworthy to mention that though the present study provides a fundamental understanding regarding the adsorption mechanism of Zn-AlNi LDH for CIP at minimal concentration, future studies focused on scale-up experiments in real-time wastewater in the presence of other co-contaminants are necessary to substantiate the economic and environmental implications. Functionalization and surface modification of adsorbents to improvise the adsorption efficiency, followed by large-scale synthesis and subsequent experiments in fixed/fluidized bed reactors to quantify the flow rate and contact time are necessary for scale-up. Techno-economic and life-cycle assessment studies are also necessary to study its long-term sustainability and feasibility during large-scale deployment.

4 Conclusion

The study explored the adsorption of CIP onto a GO-ZnAlNi LDH composite under various contact time, pH, adsorbent dosage, and initial adsorbate concentration. The composite was thoroughly characterized to determine its structural and morphological properties. Surface morphology analysis revealed the presence of ultra-thin, sheet-like structures, while XRD confirmed the crystalline nature of the GO-ZnAlNi LDH composite. The incorporation of ZnAlNi LDH into GO significantly enhanced the composite's surface area to 38.069 m^2/g, improving its adsorption efficiency for CIP. Under optimized conditions of 1 mg/L CIP concentration, 10 mg/L composite dosage, and pH 7, the maximum adsorption capacity achieved was 84.84% after 1 h. Adsorption kinetics were best described by the pseudo-first-order, Elovich kinetic models revealing the involvement of multiple surface and diffusion processes. Better fit with Freundlich isotherm further confirmed multi-layered adsorption. The findings suggest that π-π interactions and hydrogen bonding were the primary mechanisms driving CIP adsorption. The crystal structure of the composite remained intact post-adsorption, exhibiting excellent reusability, thus maintaining significant adsorption efficiency over five consecutive cycles. Overall, the potential of the synthesized GO-ZnAlNi LDH to adsorb trace levels of antibiotics (1 mg/L) from aqueous solution, even at a low adsorbent concentration of just 10 mg/L, demonstrates exceptional sensitivity, making it a superior candidate for water purification applications. Therefore, this study enhances our understanding of how antibiotics interact with GO-based composites, highlighting their significance in applying adsorption technology for treating antibiotic-contaminated wastewater. Furthermore, the applicability in real-time wastewater treatment is reinforced by the optimization of key parameters, ensuring enhanced efficiency and practical feasibility.

Data availability statement

The original contributions presented in the study are included in the article/Supplementary Material, further inquiries can be directed to the corresponding authors.

Author contributions

NS: Methodology, Writing – original draft, Data curation, Formal Analysis, Investigation, Software, Validation, Visualization. SK: Formal Analysis, Validation, Funding acquisition, Resources, Supervision, Writing – review and editing. BB: Formal Analysis, Supervision, Validation, Conceptualization, Investigation, Methodology, Project administration, Visualization, Writing – original draft. JM: Conceptualization, Formal Analysis, Investigation, Methodology, Project administration, Supervision, Validation, Visualization, Writing – review and editing, Funding acquisition, Resources, Writing – original draft.

Funding

The author(s) declare that financial support was received for the research and/or publication of this article. The authors acknowledge the financial support for this work by TIET-Centre for excellence in emerging materials (CEEMS) (TIET/CEEMS/SEED/2023/21), and TIET SEED Grant (TU/DORDC/652). Sandeep Kumar thanks Punjab Engineering College (Deemed to be University) for providing research initiation grant (No. PEC/DSR&IC/54 dated 10-04-2024) and Department of Science and Technology, Govt of India for DST-PURSE grant (No. SR/PURSE/2024/350 dated 14-10-2024).

Conflict of interest

The authors declare that the research was conducted in the absence of any commercial or financial relationships that could be construed as a potential conflict of interest.

The author(s) declared that they were an editorial board member of Frontiers, at the time of submission. This had no impact on the peer review process and the final decision.

Generative AI statement

The authors declare that no Generative AI was used in the creation of this manuscript.

Publisher's note

Supplementary material

The Supplementary Material for this article can be found online at: https://www.frontiersin.org/articles/10.3389/fnano.2025.1578620/full#supplementary-material

References

Ahmed, M. B., Zhou, J. L., Ngo, H. H., and Guo, W. (2015). Adsorptive removal of antibiotics from water and wastewater: progress and challenges. *Sci. Total Environ.* 532, 112–126. doi:10.1016/j.scitotenv.2015.05.130

Alicanoglu, P., and Sponza, D. T. (2017). Removal of ciprofloxacin antibiotic with nano graphene oxide treatment. *Desalination and Water Treatment* 63, 293–307. doi:10.5004/dwt.2017.20176

Ai, Y., Liu, Y., Huo, Y., Zhao, C., Sun, L., and Han, B. (2019). Insights into the adsorption mechanism and dynamic behavior of tetracycline antibiotics on reduced graphene oxide (RGO) and graphene oxide (GO) materials. *Environ. Sci. Nano.* 6 (11), 3336–3348. doi:10.1039/C9EN00866G

Bahar, P., Hassani, A. H., Panahi, H. A., and Moniri, E. (2021). Application of modified graphene oxide with thermosensitive polymers for adsorption of antibiotics from synthetic contaminated water. *Desalination Water Treat.* 210, 281–295. doi:10.5004/dwt.2021.26573

Bezerra, B. G. P., Bieseki, L., de Mello, M. I. S., da Silva, D. R., Rodella, C. B., and Pergher, S. (2021). Memory effect on a LDH/zeolite A composite: an XRD *in situ* study. *Materials* 14 (9), 2102. doi:10.3390/ma14092102

Bu, J., Yuan, L., Zhang, N., Meng, Y., and Peng, X. (2020). Novel adsorbent of N-phenylthiourea-functionalized graphene oxide and its removal of methyl orange in aqueous solutions. *J. Chemi. Enginee. Data*. 66 (1), 199–209. doi:10.1021/acs.jced.0c00527

Chang, L., Pu, Y., Jing, P., Cui, Y., Zhang, G., Xu, S., et al. (2021). Magnetic core-shell MnFe2O4@TiO2 nanoparticles decorated on reduced graphene oxide as a novel adsorbent for the removal of ciprofloxacin and Cu(II) from water. *Appl. Surf. Sci.* 541, 148400. doi:10.1016/j.apsusc.2020.148400

Chaturvedi, P., Shukla, P., Giri, B. S., Chowdhary, P., Chandra, R., Gupta, P., et al. (2021). Prevalence and hazardous impact of pharmaceutical and personal care products and antibiotics in environment: a review on emerging contaminants. *Environ. Res.* 194, 110664. doi:10.1016/j.envres.2020.110664

Chen, B., Li, Y., Li, M., Cui, M., Xu, W., Li, L., et al. (2021). Rapid adsorption of tetracycline in aqueous solution by using MOF-525/graphene oxide composite. *Microporous Mesoporous Mater.* 328, 111457. doi:10.1016/j.micromeso.2021.111457

Deng, J., Xiao, L., Yuan, S., Wang, W., Zhan, X., and Hu, Z.-H. (2021). Activation of peroxymonosulfate by CoFeNi layered double hydroxide/graphene oxide (LDH/GO) for the degradation of gatifloxacin. *Sep. Purif. Technol.* 255, 117685. doi:10.1016/j.seppur.2020.117685

Dixit, A., Pandey, H., Rana, R., Kumar, A., Herojeet, R., Lata, R., et al. (2024). Ecological and human health risk assessment of pharmaceutical compounds in the Sirsa River of Indian Himalayas. *Environ. Pollut.* 347, 123668. doi:10.1016/j.envpol.2024.123668

Elhaci, A., Labed, F., Khenifi, A., Bouberka, Z., Kameche, M., and Benabbou, K. (2021). MgAl-Layered double hydroxide for amoxicillin removal from aqueous media. *Int. J. Environ. Anal. Chem.* 101 (15), 2876–2898. doi:10.1080/03067319.2020.1715374

Feng, X., Long, R., Wang, L., Liu, C., Bai, Z., and Liu, X. (2022). A review on heavy metal ions adsorption from water by layered double hydroxide and its composites. *Sep. Purif. Technol.* 284, 120099. doi:10.1016/j.seppur.2021.120099

Gao, J., Zheng, X., Meng, Z., and Feng, L. (2022). Adsorption of ciprofloxacin and tetracycline from wastewater by layered double hydroxides modified vermiculite. *J. Porous Mater.* 29 (5), 1299–1308. doi:10.1007/s10934-022-01253-x

Guerrero-Contreras, J., and Caballero-Briones, F. (2015). Graphene oxide powders with different oxidation degree, prepared by synthesis variations of the Hummers method. *Mater. Chem. Phys.* 153, 209–220. doi:10.1016/j.matchemphys.2015.01.005

Han, L., Khalil, A. M. E., Wang, J., Chen, Y., Li, F., Chang, H., Zhang, H., Liu, X., Li, G., Jia, Q., and Zhang, S. (2021). Graphene-boron nitride composite aerogel: A high efficiency adsorbent for ciprofloxacin removal from water. *Separation and Purification Technology*, 278, 119605. doi:10.1016/j.seppur.2021.119605

Hidayah, N. M. S., Liu, W.-W., Lai, C.-W., Noriman, N. Z., Khe, C.-S., Hashim, U., et al. (2017). Comparison on graphite, graphene oxide and reduced graphene oxide: synthesis and characterization. *AIP Conf. Proc.* 1892 (1), 150002. doi:10.1063/1.5005764

Huang, X., Tian, J., Li, Y., Yin, X., and Wu, W. (2020). Preparation of a three-dimensional porous graphene oxide–kaolinite–poly(vinyl alcohol) composite for efficient adsorption and removal of ciprofloxacin. *Langmuir* 36 (37), 10895–10904. doi:10.1021/acs.langmuir.0c00654

Johnston, A.-L., Lester, E., Williams, O., and Gomes, R. L. (2024). Interactions between antibiotic removal, water matrix characteristics and layered double hydroxide sorbent material. *Chemosphere* 367, 143546. doi:10.1016/j.chemosphere.2024.143546

Kanimozhi, S. N., Aljafari, B., Singh, R., Anandan, S., and Ashokkumar, M. (2023). Rod-like manganese–cobalt layered double hydroxides for the development of supercapacitor electrodes. *Nano-Structures & Nano-Objects* 36, 101044. doi:10.1016/j.nanoso.2023.101044

Khan, N. A., Najam, T., Shah, S. S. A., Hussain, E., Ali, H., Hussain, S., et al. (2020). Development of Mn-PBA on GO sheets for adsorptive removal of ciprofloxacin from water: kinetics, isothermal, thermodynamic and mechanistic studies. *Mater. Chem. Phys.* 245, 122737. doi:10.1016/j.matchemphys.2020.122737

Khorshidi, M., Asadpour, S., Sarmast, N., Aramesh-Boroujeni, Z., and Sadegh, N. (2023). Enhanced adsorption performance of tetracycline in aqueous solutions using Mg-Al-LDH/AC nanocomposite. *Arabian J. Chem.* 16 (12), 105301. doi:10.1016/j.arabjc.2023.105301

Kovalakova, P., Cizmas, L., McDonald, T. J., Marsalek, B., Feng, M., and Sharma, V. K. (2020). Occurrence and toxicity of antibiotics in the aquatic environment: A review. Chemosphere, 251, 126351. doi:10.1016/j.chemosphere.2020.126351

Li, K., Ou, H., Zhou, D., Gong, C., Xue, H., and Li, Y. (2021). Study of the removal of ciprofloxacin by Zn–GO@SA aerogel microspheres. *New J. Chem.* 45 (7), 3630–3639. doi:10.1039/D0NJ05639A

Li, M., Liu, Y., Liu, S., Zeng, G., Hu, X., Tan, X., et al. (2018). Performance of magnetic graphene oxide/diethylenetriaminepentaacetic acid nanocomposite for the tetracycline and ciprofloxacin adsorption in single and binary systems. *J. Colloid Interface Sci.* 521, 150–159. doi:10.1016/j.jcis.2018.03.003

Mohammadi, L., Rahdar, A., Khaksefidi, R., Ghamkhari, A., Fytianos, G., and Kyzas, G. Z. (2020). Polystyrene magnetic nanocomposites as antibiotic adsorbents. *Polymers* 12 (6), 1313. doi:10.3390/polym12061313

Parashar, D., Harafan, A., Achari, G., and Kumar, M. (2023). Ciprofloxacin and metronidazole adsorption on chitosan-modified graphene oxide as single-compound and binary mixtures: kinetics, isotherm, and sorption mechanism. *J. Hazard. Toxic, Radioact. Waste* 27 (1), 04022042. doi:10.1061/(ASCE)HZ.2153-5515.0000724

Phoon, B. L., Ong, C. C., Mohamed Saheed, M. S., Show, P.-L., Chang, J.-S., Ling, T. C., et al. (2020). Conventional and emerging technologies for removal of antibiotics from wastewater. *J. Hazard. Mater.* 400, 122961. doi:10.1016/j.jhazmat.2020.122961

Priyanka, P., Pal, B., Singh, S., and Bansal, M. (2024). Superior adsorptive removal of ciprofloxacin by graphene oxide modified Ni-Al layered double hydroxide composites. *J. Alloys Compd.* 976, 173220. doi:10.1016/j.jallcom.2023.173220

Rahman, N., and Raheem, A. (2022). Graphene oxide/Mg-Zn-Al layered double hydroxide for efficient removal of doxycycline from water: Taguchi approach for optimization. *J. Molecu. Liqu.* 354, 118899. doi:10.1016/j.molliq.2022.118899

Radmehr, S., Hosseini Sabzevari, M., Ghaedi, M., Ahmadi Azqhandi, M. H., and Marahel, F. (2021). Adsorption of nalidixic acid antibiotic using a renewable adsorbent based on Graphene oxide from simulated wastewater. *J. Environ. Chem. Eng.* 9 (5), 105975. doi:10.1016/j.jece.2021.105975

Rashed, S. H., Abd-Elhamid, A. I., Abdalkarim, S. Y. H., El-Sayed, R. H., El-Bardan, A. A., and Soliman, H. M. (2022). Preparation and characterization of layered-double hydroxides decorated on graphene oxide for dye removal from aqueous solution. *J. Materi. Res. Technol.* 17, 2795. doi:10.1016/j.jmrt.2022.02.040

Shahnaz, T., Bedadeep, D., and Narayanasamy, S. (2022). Investigation of the adsorptive removal of methylene blue using modified nanocellulose. *Int. J. Biol. Macromol.* 200, 162–171. doi:10.1016/j.ijbiomac.2021.12.081

Shahnaz, T., Mohamed Madhar, F. S., Padmanaban, V. C., and Narayanasamy, S. (2020). Surface modification of nanocellulose using polypyrrole for the adsorptive removal of Congo red dye and chromium in binary mixture. *Int. J. Biol. Macromol.* 151, 322–332. doi:10.1016/j.ijbiomac.2020.02.181

Sharma, V., Shahnaz, T., Subbiah, S., and Narayanasamy, S. (2020). New insights into the remediation of water pollutants using nanobentonite incorporated nanocellulose chitosan based aerogel. *J. Polym. Environ.* 28 (7), 2008–2019. doi:10.1007/s10924-020-01740-9

Singh, S., Naik, T. S. S. K., Shehata, N., Aguilar-Marcelino, L., Dhokne, K., Lonare, S., et al. (2023). Novel insights into graphene oxide-based adsorbents for remediation of hazardous pollutants from aqueous solutions: a comprehensive review. *J. Mol. Liq.* 369, 120821. doi:10.1016/j.molliq.2022.120821

Stobinski, L., Lesiak, B., Malolepszy, A., Mazurkiewicz, M., Mierzwa, B., Zemek, J., et al. (2014). Graphene oxide and reduced graphene oxide studied by the XRD, TEM and electron spectroscopy methods. *J. Electron Spectrosc. Relat. Phenom.* 195, 145–154. doi:10.1016/j.elspec.2014.07.003

Sun, L. (2019). Structure and synthesis of graphene oxide. *Chin. J. Chem. Eng.* 27 (10), 2251–2260. doi:10.1016/j.cjche.2019.05.003

Tang, Y., Guo, H., Xiao, L., Yu, S., Gao, N., and Wang, Y. (2013). Synthesis of reduced graphene oxide/magnetite composites and investigation of their adsorption performance of fluoroquinolone antibiotics. *Colloids Surfaces A Physicochem. Eng. Aspects* 424, 74–80. doi:10.1016/j.colsurfa.2013.02.030

Tao, J., Yang, J., Ma, C., Li, J., Du, K., Wei, Z., et al. (2020). Cellulose nanocrystals/graphene oxide composite for the adsorption and removal of levofloxacin hydrochloride antibiotic from aqueous solution. *R. Soc. Open Sci.* 7 (10), 200857. doi:10.1098/rsos.200857

Tasrin, S., Mohamed Madhar Fazil, S., Senthilmurugan, S., and Selvaraju, N. (2021). Facile preparation of nanocellulose embedded polypyrrole for dye removal: unary and binary process optimization and seed toxicity. *Int. J. Environ. Sci. Technol.* 18 (2), 365–378. doi:10.1007/s13762-020-02814-w

Upoma, B. P., Yasmin, S., Ali Shaikh, M. A., Jahan, T., Haque, M. A., Moniruzzaman, M, et al. (2022). A fast adsorption of azithromycin on waste-product-derived graphene oxide induced by H-bonding and electrostatic interactions. *ACS Omega* 7 (34), 29655–29665. doi:10.1021/ACSOMEGA.2C01919/ASSET/IMAGES/LARGE/AO2C01919_0008.JPEG

Wang, F., Yang, B., Wang, H., Song, Q., Tan, F., and Cao, Y. (2016). Removal of ciprofloxacin from aqueous solution by a magnetic chitosan grafted graphene oxide composite. *J. Mol. Liq.* 222, 188–194. doi:10.1016/j.molliq.2016.07.037

Wang, G., Huang, D., Cheng, M., Chen, S., Zhang, G., Lei, L., et al. (2022). Metal-organic frameworks template-directed growth of layered double hydroxides: a fantastic conversion of functional materials. *Coord. Chem. Rev.* 460, 214467. doi:10.1016/j.ccr.2022.214467

Wang, J., Yao, Q., Sheng, C., Jin, C., and Sun, Q. (2017). One-step preparation of graphene oxide/cellulose nanofibril hybrid aerogel for adsorptive removal of four kinds of antibiotics. *J. Nanomater.* 2017 (1), 1–10. doi:10.1155/2017/5150613

Yasmin, S., Azam, M. G., Hossain, M. S., Akhtar, U. S., and Kabir, M. H. (2024). Efficient removal of ciprofloxacin from aqueous solution using Zn–C battery derived graphene oxide enhanced by hydrogen bonding, electrostatic and π-π interaction. *Heliyon* 10 (12), e33317. doi:10.1016/j.heliyon.2024.e33317

Yu, F., Li, Y., Han, S., and Ma, J. (2016). Adsorptive removal of antibiotics from aqueous solution using carbon materials. *Chemosphere* 153, 365–385. doi:10.1016/j.chemosphere.2016.03.083

Zhou, Y., Cao, S., Xi, C., Li, X., Zhang, L., Wang, G., et al. (2019). A novel Fe3O4/graphene oxide/citrus peel-derived bio-char based nanocomposite with enhanced adsorption affinity and sensitivity of ciprofloxacin and sparfloxacin. *Bioresour. Technol.* 292, 121951. doi:10.1016/j.biortech.2019.121951

Zhu, X., Tsang, D. C. W., Chen, F., Li, S., and Yang, X. (2015). Ciprofloxacin adsorption on graphene and granular activated carbon: kinetics, isotherms, and effects of solution chemistry. *Environ. Technol.* 36 (24), 3094–3102. doi:10.1080/09593330.2015.1054316